Journal of Molecular Liquids 365 (2022) 120217

Contents lists available at ScienceDirect

Journal of Molecular Liquids

journal homepage: www.elsevier.com/locate/molliq

Synthesis and structure-activity-toxicity relationships of DABCO-containing ammonium amphiphiles based on natural isatin scaffold

T.N. Pashirova [a,*], Z.M. Shaihutdinova [a], A.E. Vandyukov [a], A.P. Lyubina [a], S.K. Amerhanova [a], A.D. Voloshina [a], A.V. Samorodov [b], E.B. Souto [c,d], V.F. Mironov [a], A.V. Bogdanov [a,*]

[a] Arbuzov Institute of Organic and Physical Chemistry, FRC Kazan Scientific Center, Russian Academy of Sciences, Arbuzov St., 8, Kazan 420088, Russian Federation
[b] Bashkir State Medical University, Ufa 450000, Russian Federation
[c] Department of Pharmaceutical Technology, Faculty of Pharmacy of University of Porto, R. Jorge de Viterbo Ferreira 228, 4050-313 Porto, Portugal
[d] REQUIMTE/UCIBIO, Faculty of Pharmacy of University of Porto, R. Jorge de Viterbo Ferreira 228, 4050-313 Porto, Portugal

ARTICLE INFO

Article history:
Received 9 June 2022
Revised 23 August 2022
Accepted 24 August 2022
Available online 29 August 2022

Keywords:
Quaternary ammonium compounds
Isatin
Self-assembly
π-Amphiphiles
Critical association concentration
Surfactants
Solubilization
Antimicrobial activity

ABSTRACT

This work deals with the creation of new multifunctional quaternary ammonium compounds (QACs) on natural isatin scaffold as a new generation of antimicrobial agents. 1-R-isatin-3-acylhydrazones containing quaternized DABCO moieties (Dabco-Is-n) with varying hydrophobicity (R = C_nH_{2n+1}, where n = 10, 12, 14, 16, 18) were synthesized. The idea was to combine two bactericidal fragments, presumably with different mechanisms of action, in the structure of self-assembling quaternary ammonium compounds. The self-assembly behavior, solubility properties toward hydrophobic dye Sudan I, antimicrobial activity against gram-positive and gram-negative bacteria, fungi, hemolytic activity, cell toxicity (MTT-test) and *in vitro* anticoagulant and anti-aggregation activities were investigated. Established by tensiometry, conductometry, dynamic light scattering and UV-spectrophotometry, the value of Dabco-Is-n critical micelle concentration is 10 times lower than for Dabco-n surfactants. That is, Dabco-Is-n self-assemblies are responsible factor for the manifestation of antimicrobial activity. Dabco-Is-12 was found to be largely blood biocompatible with low toxicity and low hemolysis (IC_{50} and HC_{50} are $\geq$ 100 μM, negligible coagulation) and with high biological activity against methicillin-resistant strains of *S. aureus* MRSA-1 and MRSA-2 (MIC = 3.5 and 7.0 μM, respectively) and high solubilization capacity toward hydrophobic dye (Sudan I). Moreover, it forms hydrogen-bonds with drugs (niclosamide and piperine) and displays a good selectivity index toward fungi *Candida albicans ATCC 10231*. Such new nontoxic Dabco-Is-n biocides with antibacterial and antifungal effects have a good potential for medical applications.

1. Introduction

The widespread use of quaternary ammonium compounds (QAC) from industry to biomedicine is caused by the decisive role of their structures, namely, a positively charged head and an alkyl hydrophobic chain [1,2]. This enables electrostatic interactions with negative charged surfaces, and determine numerous applications ranging from anti-corrosion, anti-static agents, air conditioners to biocides [3,4] and gene transfectors [5], paying particular attention to maintain balance between high activity and biocompatibility of these molecules. In this regard, the toxicological aspect of QAC is given priority for both living organisms and the environment. Therefore, more and more studies of QAC are aimed at their structure–activity-toxicity relationships [1,6,7] and their selectivity towards bacterial and mammalian cells. A common strategy is to design building blocks for creating QAC with an optimal hydrophilic-lipophilic balance and properties [8]. One of the first approaches is the creation of dimeric or gemini surfactants containing two head groups and two alkyl fragments, exhibiting their unique properties at low threshold concentrations, and

Abbreviations: QACs, quaternary ammonium compounds; DABCO, 1,4-diazabicyclo[2.2.2]octane; Dabco-Is-n, Isatin-3-acylhydrazones containing quaternized DABCO moieties; Is-n, Isatin-3-acylhydrazones containing a trimethylammonium moiety; CMC, critical micelle concentration; CTAB, hexadecyltrimethylammonium bromide; HLB, hydrophilic-lipophilic balance.

* Corresponding authors.
E-mail addresses: tatyana_pashirova@mail.ru (T.N. Pashirova), abogdanov@inbox.ru (A.V. Bogdanov).

https://doi.org/10.1016/j.molliq.2022.120217
0167-7322/

therefore at lower and less toxic doses [9,10]. Another approach is the incorporation of biodegradable or cleavable moieties into the structure of QAC, e.g. amide and ester groups [11], amino acid [12–14], purine and pyrimidine bases [15], glycosides and nucleoside [16,17], phenylalaninyl-proline dipeptide [18]. Such compounds are environment-friendly or green surfactants. An additional well-known way to reduce the toxicity of QACs is the design of alkyl-substituted salts containing natural anions, such as glycolate, D-gluconate, α-ketoglutarate, L-pyroglutamate and cholate [19,20].

Recent trend in environmentally sustainable is natural product derivatization and creation of biocompatible, less toxic QACs on scaffolds of natural products, for example, such as alkaloids, terpenoids, acetylenes, coumarins, etc. [21–27]. They are also classified as multifunctional compounds showing broad spectrum antimicrobial activity [28] including anti-biofilm properties, and as well as environmentally friendly surfactant [29].

Usually, QACs show a non-linear dependence of biological activity on the length of their alkyl chain. The maximum biological activity is observed for QAC with 12–14 carbon atoms [30]. Thus, lipophilicity is a critical factor for efficiency of self-assembling QAC, but does not appear to be the exclusive factor influencing antimicrobial activity [31]. For example, heterocyclic ammonium salts based on the benzimidazole skeleton exhibited a different antibacterial mechanism of action. They do not only target the bacterial membrane, but also bind to cellular macromolecules [32].

The current theories of microbial cell destruction mechanism involve formation of QAC self-assemblies at low concentrations. The positive charge and the local concentration of QAC near the bacterial membrane are more effectively increased by binding of a complex QAC supramolecular self-assemblies compared to a single QAC molecules [32]. Probably, supramolecular mechanism" of QAC self-assemblies is similar to the action of biosurfactants [33,34].

In our work, two bactericidal fragments, presumably with different mechanisms of action were combined in the structure of self-assembled QAC. Such new biocides may have antibacterial and antifungal actions towards a wide range of pathogens. Thus, heterocyclic compounds containing an isatin moiety possess antimicrobial, antiviral, antitubercular, anti-HIV, antitumor, and anticonvulsant activities [35–42]. They include kinase inhibition for tumor treatment, inhibition/modulation of proteases, translation initiation, neovascularisation, and tubulin polymerization [43,44]. Their biological activity was modulated by hydrophilic-lipophilic balance of π-amphiphiles and their tunable self-assembly behavior [45]. QACs with more rigidly disposed side chains, such as those in 1,4-diazabicyclo[2.2.2]octane (DABCO) showed the highest level of antimicrobial activity and rather high therapeutic index [46,47]. In addition, DABCO is highly reactive and not an expensive compound. There are numerous possibilities for their molecular design; in particular, they can be used to obtain new lipophilic compounds containing one, two, and four charged nitrogen atoms [48,49]. It is known that a saturated bicyclic framework with one nitrogen atom (quinuclidine) occurs in natural physiologically active substances [50]. DABCO-long-chain amphiphile displays lower toxicity than the hexadecyltrimethylammonium bromide (CTAB) and unusual biological activity with a maximum for the C18-chain compound [51]. DABCO-amphiphile mixture with the antimicrobial drug furazolidone makes to obtain non-toxic antimicrobial compositions [52].

The aim of this work was the synthesis of new environmentally benign amphiphilic quaternary ammonium compounds based on natural isatin scaffold in combination with DABCO fragment. The establishment of a structure-biological activity relationship, depending on the length of the hydrophobic chain in oxindole fragment and the nature of the substituent in the benzene ring was given.

2. Materials and methods

2.1. Materials

1-(*o*-Tolylazo)-2-naphthol (75 %, Orange OT, Aldrich, USA), 1,4-diazabicyclo[2.2.2]octane (>99 %, Sigma-Aldrich, USA), 5-chloroisatin (97 %, Sigma-Aldrich, USA), trifluoroacetic acid (≥99 %, Sigma-Aldrich, USA) were used as received. Isatin derivatives (**1a,b,d-g**) [53–55] and hydrazide (2) were synthesized according to previously described procedures [56].

2.2. Synthesis and characterization of novel isatin derivative (*1c*) and ammonium salts (*3a-g*)

*2.2.1 5-Chloro-1-decylindoline-2,3-dione (**1c**).* To a magnetically stirred solution of 5-chloro-isatin (0.91 g, 5 mmol) in dry DMF (15 ml) NaH (0.21 g, 5 mmol, 60 % suspension in mineral oil) was added in small portions at 10 °C. After 30 min to a dark violet reaction mixture 1-bromodecane (1.04 ml, 5 mmol) was added followed by additional stirring at room temperature (25 °C) for 1 h and for 3 h at 60 °C. Then the solution was poured into a mixture of crushed ice/water (200 ml), the precipitate that formed was filtered off, washed consecutively with water (50 ml), petroleum ether (20 ml) and dried in vacuo.

Orange powder. Yield: 73 %; m.p. 60 °C. **IR (KBr, cm^{-1})**: 2922 (C—H), 2851 (C—H), 1732 (C=O), 1605 (C=C). **^{1}H NMR (400 MHz, $CDCl_3$, δ, ppm)**: 0.87 (t, *J* = 7.0 Hz, 3H), 1.25–1.37 (m, 14H), 1.64–1.71 (m, 2H), 3.70 (t, *J* = 7.3 Hz, 2H), 6.85 (dd, *J* = 8.2 Hz, 0.5 Hz, 1H), 7.53–7.56 (m, 2H). **^{13}C NMR (100 MHz, $CDCl_3$, δ, ppm)**: 182.60, 157.57, 149.34, 137.59, 129.41, 125.33, 118.44, 111.39, 40.44, 31.82, 29.44, 29.41, 29.22, 29.16, 27.16, 26.84, 22.62, 14.05. **ESI MS**: *m*/*z* 344.2 [M + Na]$^+$; **Anal.Calc.for** $C_{18}H_{24}ClNO_2$; C, 67.17; H, 7.52; Cl, 11.01; N, 4.35; found, C, 67.02; H, 7.65; Cl, 10.90; N, 4.28.

2.2.2 General procedure for the synthesis of 1-(2-(2-(1-alkyl-2-oxoindolin-3-ylidene)hydrazinyl)-2-oxoethyl)-1,4-diazabicyclo[2.2.2]octan-1-ium bromides (Dabco-Is-n). A mixture of substituted isatin **1a-g** (1 mmol) and hydrazide **2** (1 mmol) was magnetically stirred in absolute ethanol (7 ml) for 10 min followed by addition of trifluoroacetic acid (20 mol%). Then the reaction mixture was heated at reflux for 3 h. After cooling the solution to room temperature, solvent was rotary evaporated. The precipitate that formed was washed with anhydrous diethyl ether, filtered off and dried in vacuum (12 Torr) at 60 °C.

1-(2-(2-(1-Decyl-2-oxoindolin-3-ylidene)hydrazinyl)-2-oxoethyl)-1,4-diazabicyclo[2.2.2]octan-1-ium bromide (**Dabco-Is-10**).

Yellow powder. Yield: 87 %; m.p. 260 °C. **IR (KBr, cm^{-1})**: 3443 (N—H), 3219 (N—H), 2925 (C—H), 2853 (C—H), 1708 (C=O), 1677 (C=O), 1616 (C=C), 1468 (C=N). **^{1}H NMR (600 MHz, $CDCl_3$/DMSO d_6 1:2, δ, ppm)**: 0.83 (t, *J* = 7.1 Hz, 3H), 1.21–1.30 (m, 14H), 1.61–1.67 (m, 2H), 3.30 (br. s, overlapped with H_2O signal), 3.73 (t, *J* = 7.3 Hz, 2H), 3.81 (br. s, 6H), 4.94 (s, 2H), 7.09–7.16 (m, 2H), 7.45 (dd, *J* = 7.7 Hz, 7.6 Hz, 1H), 7.63–7.66 (m, 1H), 12.73 s (1H, NH). **^{13}C NMR (150 MHz, $CDCl_3$/DMSO d_6 1:2, δ, ppm)**: 165.24, 159.22, 143.23, 132.06, 127.52, 122.88, 120.90, 119.08, 109.87, 59.85, 52.18, 44.09, 39.21, 31.12, 28.77, 28.75, 28.51, 28.48, 26.75, 26.13, 21.93, 13.69. **ESI MS**: *m*/*z* 454.4 [M−Br]$^+$; **Anal.Calc.for** $C_{26}H_{40}BrN_5O_2$; C, 58.42; H, 7.54; Br, 14.95; N, 13.10; found, C, 58.30; H, 7.46; Br, 14.81; N, 13.01.

1-(2-(2-(1-Decyl-5-methyl-2-oxoindolin-3-ylidene)hydrazinyl)-2-oxoethyl)-1,4-diazabicyclo[2.2.2]octan-1-ium bromide (**Dabco-Is-CH_3-10**).

Yellow powder. Yield: 82 %; m.p. 232 °C (dec.). **IR (KBr, cm^{-1})**: 3343 (N—H), 3196 (N—H), 2923 (C—H), 2853 (C—H), 1679 (C=O), 1612 (C=C), 1467 (C=N). **^{1}H NMR (600 MHz, DMSO d_6, δ, ppm)**:

0.84 (t, *J* = 7.1 Hz, 3H), 1.22–1.27 (m, 14H), 1.58–1.63 (m, 2H), 3.10–3.16 (m, 8H), 3.66 (br. s, 6H), 3.73 (t, *J* = 6.9 Hz, 2H), 4.87 (s, 2H), 7.24 (d, *J* = 8.4 Hz, 1H), 7.67 (dd, *J* = 8.3 Hz, 1.6 Hz, 1H), 7.87–7.89 (m, 1H), 12.58 (s, 1H, NH). **^{13}C NMR (150 MHz, DMSO d_6, δ, ppm)**: 165.68, 160.03, 142.50, 134.31, 134.04, 123.37, 120.76, 114.95, 112.39, 59.68, 52.60, 52.52, 44.38, 40.04, 31.16, 28.78, 28.75, 28.54, 28.48, 26.69, 26.03, 21.98, 13.85. **MALDI MS**: *m*/*z* 468.4 [M−Br]$^+$; **Anal.Calc.for** $C_{27}H_{42}BrN_5O_2$; C, 59.12; H, 7.72; Br, 14.57; N, 12.77; found, C, 59.00; H, 7.59; Br, 14.40; N, 12.61.

1-(2-(2-(5-Chloro-1-decyl-2-oxoindolin-3-ylidene)hydrazinyl)-2-oxoethyl)-1,4-diazabicyclo[2.2.2]octan-1-ium bromide (**Dabco-Is-Cl-10**).

Yellow powder. Yield: 95 %; m.p. 233 °C (dec.). **IR (KBr, cm^{-1})**: 3587 (N—H), 3193 (N—H), 2924 (C—H), 2853 (C—H), 1719 (C=O), 1682 (C=O), 1614 (C=C), 1451 (C=N). **^{1}H NMR (600 MHz, DMSO d_6, δ, ppm)**: 0.84 (t, *J* = 7.0 Hz, 3H), 1.22–1.28 (m, 14H), 1.58–1.63 (m, 2H), 3.10 (t, *J* = 7.2 Hz, 6H), 3.51 (t, *J* = 7.2 Hz, 6H), 3.74 (t, *J* = 6.9 Hz, 2H), 4.86 (s, 2H), 7.29 (d, *J* = 8.4 Hz, 1H), 7.55 (dd, *J* = 8.5 Hz, 1.8 Hz, 1H), 7.76–7.79 (m, 1H), 12.58 (br. s (1H, NH). **^{13}C NMR (150 MHz, DMSO d_6, δ, ppm)**: 165.70, 161.13, 142.11, 134.20, 131.50, 127.35, 120.65, 120.39, 111.96, 61.39, 52.54, 44.40, 40.03, 31.16, 28.77, 28.75, 28.53, 28.48, 26.70, 26.03, 21.97, 13.84. **ESI MS**: *m*/*z* 488.3 [M−Br]$^+$; **Anal.Calc.for** $C_{26}H_{39}BrClN_5O_2$; C, 54.88; H, 6.91; Br, 14.04; Cl, 6.23; N, 12.31; found, C, 54.70; H, 6.78; Br, 13.93; Cl, 6.11; N, 12.25.

1-(2-(2-(1-Dodecyl-2-oxoindolin-3-ylidene)hydrazinyl)-2-oxoethyl)-1,4-diazabicyclo[2.2.2]octan-1-ium bromide (**Dabco-Is-12**).

Yellow powder. Yield: 93 %; m.p. 195 °C. **IR (KBr, cm^{-1})**: 3399 (N—H), 3245 (N—H), 2925 (C—H), 2853 (C—H), 1709 (C=O), 1677 (C=O), 1616 (C=C), 1467 (C=N). **^{1}H NMR (600 MHz, $CDCl_3$/DMSO d_6 2:1, δ, ppm)**: 0.79 (t, *J* = 7.0 Hz, 3H), 1.17–1.26 (m, 16H), 1.59–1.62 (m, 2H), 3.45 (br. s, 6H), 3.64 (br. s, 4H), 4.18 (br. s, 6H), 5.17 (s, 2H), 6.85 (d, *J* = 7.8 Hz, 1H), 7.04–7.08 (m, 1H), 7.33–7.37 (m, 1H), 7.69 (d, *J* = 6.6 Hz, 1H), 12.75 s (1H, NH). **^{13}C NMR (150 MHz, $CDCl_3$/DMSO d_6 2:1, δ, ppm)**: 164.77, 160.20, 142.95, 135.63, 131.80, 122.94, 121.57, 118.07, 109.03, 60.01, 51.87, 44.11, 34.10, 28.84, 28.81, 28.75, 28.72, 28.56, 28.50, 28.46, 26.72, 26.17, 21.91, 13.46. **MALDI MS**: *m*/*z* 482.4 [M−Br]$^+$; **Anal.Calc.for** $C_{28}H_{44}BrN_5O_2$; C, 59.78; H, 7.88; Br, 14.20; N, 12.45; found, C, 59.60; H, 7.75; Br, 14.05; N, 12.33.

1-(2-(2-(1-Tetradecyl-2-oxoindolin-3-ylidene)hydrazinyl)-2-oxoethyl)-1,4-diazabicyclo[2.2.2]octan-1-ium bromide (**Dabco-Is-14**).

Yellow powder. Yield: 96 %; m.p. 182 °C. **IR (KBr, cm^{-1})**: 3400 (N—H), 3225 (N—H), 2922 (C—H), 2853 (C—H), 1708 (C=O), 1677 (C=O), 1617 (C=C), 1467 (C=N). **^{1}H NMR (600 MHz, DMSO d_6, δ, ppm)**: 0.84 (t, *J* = 7.1 Hz, 3H), 1.22–1.28 (m, 22H), 1.59–1.65 (m, 2H), 3.22 (br. s, 6H), 3.67–3.74 (m, 8H), 4.93 (s, 2H), 6.85 (d, *J* = 7.8 Hz, 1H), 7.17–7.22 (m, 1H), 7.23 (d, *J* = 7.4 Hz, 1H), 7.67–7.71 (m, 1H), 12.68 (s, 1H, NH). **^{13}C NMR (150 MHz, DMSO d_6, δ, ppm)**: 165.57, 160.42, 143.39, 135.31, 132.27, 123.10, 121.03, 118.48, 110.29, 59.77, 52.40, 44.22, 40.03, 28.92, 28.89, 28.84, 28.77, 28.59, 28.51, 26.78, 26.10, 21.88, 13.83. **MALDI MS**: *m*/*z* 510.4 [M−Br]$^+$; **Anal.Calc.for** $C_{30}H_{48}BrN_5O_2$; C, 61.01; H, 8.19; Br, 13.53; N, 11.86; found, C, 60.89; H, 8.02; Br, 13.36; N, 11.60.

1-(2-(2-(1-Hexadecyl-2-oxoindolin-3-ylidene)hydrazinyl)-2-oxoethyl)-1,4-diazabicyclo[2.2.2]octan-1-ium bromide (**Dabco-Is-16**).

Yellow powder. Yield: 97 %; m.p. 135 °C. **IR (KBr, cm^{-1})**: 3400 (N—H), 3203 (N—H), 2919 (C—H), 2851 (C—H), 1706 (C=O), 1675 (C=O), 1616 (C=C), 1468 (C=N). **^{1}H NMR (600 MHz, $CDCl_3$, δ, ppm)**: 0.87–0.89 (m, 3H), 1.25–1.32 (m, 26H), 1.62–1.68 (m, 2H), 3.31 (br. s, 6H), 3.63–3.67 (m, 2H), 4.20 (br. s, 6H), 5.35 (s, 2H), 6.81–6.84 (m, 1H), 7.12–7.16 (m, 1H), 7.35–7.40 (m, 1H), 7.92–7.95 (m, 1H), 12.76 (s, 1H, NH). **^{13}C NMR (150 MHz, DMSO d_6, δ, ppm)**: 165.53, 160.45, 143.42, 135.32, 132.30, 123.12, 121.02, 118.51, 110.35, 59.88, 52.26, 43.98, 40.03, 31.19, 28.91, 28.90, 28.84, 28.77, 28.59, 28.51, 26.78, 26.11, 21.98, 13.84. **MALDI MS**: *m*/*z* 538.5 [M−Br]$^+$; **Anal.Calc.for** $C_{32}H_{52}BrN_5O_2$; C, 62.12; H, 8.47; Br, 12.91; N, 11.32; found, C, 62.01; H, 8.35; Br, 12.87; N, 11.27.

1-(2-(2-(1-Octadecyl-2-oxoindolin-3-ylidene)hydrazinyl)-2-oxoethyl)-1,4-diazabicyclo[2.2.2]octan-1-ium bromide (**Dabco-Is-18**).

Yellow powder. Yield: 98 %; m.p. 210 °C. **IR (KBr, cm^{-1})**: 3432 (N—H), 3232 (N—H), 2920 (C—H), 2851 (C—H), 1710 (C=O), 1676 (C=O), 1616 (C=C), 1468 (C=N). **^{1}H NMR (400 MHz, DMSO d_6, δ, ppm)**: 0.85 (t, *J* = 6.7 Hz, 3H), 1.22–1.28 (m, 30H), 1.60–1.65 (m, 2H), 3.11 (br. s, 6H), 3.63 (br. s, 6H), 3.74 (t, *J* = 6.7 Hz, 2H), 4.85 (s, 2H), 7.17–7.24 (m, 2H), 7.48–7.52 (m, 1H), 7.64–7.69 (m, 1H), 12.69 (s, 1H, NH). **^{13}C NMR (100 MHz, DMSO d_6, δ, ppm)**: 165.96, 160.65, 143.47, 132.29, 128.65, 123.13, 121.00, 117.83, 110.17, 69.97, 52.64, 44.49, 31.21, 28.92, 28.79, 28.61, 28.72, 28.52, 26.79, 26.12, 22.00, 13.85. **MALDI MS**: *m*/*z* 566.5 [M−Br]$^+$; **Anal.Calc.for** $C_{34}H_{56}BrN_5O_2$; C, 63.14; H, 8.73; Br, 12.35; N, 10.83; found, C, 63.07; H, 8.65; Br, 12.25; N, 10.73.

2.3. NMR spectroscopy

^{1}H and ^{13}C NMR spectra were recorded on a Bruker Avance-400 or Bruker Avance-600 spectrometers at 400, 600 and 100, 150 MHz, respectively. Chemical shifts were reported in ppm relative to residual signals of protons of deuterated solvents. $CDCl_3$ or D_2O/DMSO d_6 were used as NMR solvents.

2.4. MALDI spectrometry

MALDI mass spectra were recorded on an UltraFlex III TOF/TOF mass spectrometer in linear mode with recording of positive ions, metal target, and *para*-nitroaniline matrix. Nd laser: YAG, λ 355 nm. Data were processed with the FlexAnalysis 3.0 software.

2.5. Tensiometry

Surface tension measurements were performed using the du Nouy ring detachment method (Kruss K6 Tensiometer, Hamburg, Germany). Briefly, the spherical ring was placed parallel to the air/-solvent interface. Between two surface tension analyses, the ring was cleaned with Ultra-purified water, followed by soaking in ethanol for 5–7 min, rinsing again with Ultra-purified water, and finally flame-drying. Temperature was maintained constant at 25 °C during all measurements.

2.6. Conductometry

Specific conductivity was measured using a WTW InoLabCond 720 precision conductivity meter (WTW Gmb, Weilheim, Germany). Reproducibility was checked for samples, and no significant differences were observed. All samples were studied at constant temperature, 25 °C. Purified water (18.2 MΩ cm resistivity at 25 °C) from Direct-Q 5 UV equipment (Millipore S.A.S. 67,120 Molsheim-France) was used for all sample preparations.

2.7. Dynamic light scattering

Size, zeta potential and polydispersity index of nanoparticles were determined by dynamic light scattering (DLS) measurements, using the Malvern Instrument Zetasizer Nano (Worcestershire, UK). Measured autocorrelation functions were analyzed by Malvern DTS software, applying the second-order cumulant expansion methods. The effective hydrodynamic radius (R_H) was calculated according to the Einstein-Stokes equation $D = k_BT/6\pi\eta R_H$, where

D is the diffusion coefficient, k_B the Boltzmann constant, T the absolute temperature, and η the viscosity. The diffusion coefficient was measured at least in triplicate for each sample. The average error of measurements was ± 4 %. All samples were diluted with ultra-purified water to suitable concentration and analyzed in triplicate.

2.8. UV spectrophotometry (Dye solubilization)

Solubilization of the dye (Sudan I) was performed by adding an excess of crystalline Sudan I to Dabco-Is-n solutions. These solutions were allowed to equilibrate for about 48 h at constant temperature (25 °C), followed by filtration. UV absorbance was measured using PerkinElmer λ35 (PerkinElmer Instruments, USA) at 485 nm (for Sudan I). Quartz cuvettes (1 cm containing sample were used. Solubilization capacity of Dabco-Is-n associates (S), which corresponds to the number of moles of dye solubilized per mole of Dabco-Is-n was determined according to equation (1) [57]:

$$S = B/(\varepsilon_{ext} \times l) \quad (1)$$

where B is the slope of dye absorbance as a function of surfactant concentration above CAC, and ε_{ext} the extinction coefficient of Sudan (ε_{ext} = 8700 M^{-1} cm^{-1}) [52].

2.9. IR spectroscopy

Infrared spectra were measured with a Bruker Tensor-27 instrument for the solid samples in KBr pellets. Concentration of amphiphile was kept at 19 mM (10 mg/mL) in each case. 0.07 mm CaF_2 cell was used for carrying out experiments on self-assembled state of Dabco-Is-16 and Dabco-Is-12. Micrographs of the samples in polarized light were obtained using a combined IR and optical microscope Hyperion 2000 Bruker.

2.10. Antimicrobial activity

Antimicrobial activity of the test-compounds was determined by the serial dilution technique in Muller Hinton Broth 2 and in Sabouradu broth for fungi. The cultures used for testing included Gram-positive bacteria: *Staphylococcus aureus ATCC 6538P FDA 209P*, *Bacillus cereus ATCC 10,702 NCTC 8035, Enterococcus faecalis ATCC 29212*; Gram-negative bacteria: *Escherichia coli ATCC 25922*, *Pseudomonas aeruginosa* ATCC 9027, and fungi: *Trichophyton mentagrophytes* var. gypseum 1773, and *Candida albicans ATCC 10231*; methicillin-resistant strains of *S. aureus* (MRSA) was obtained from hospital patients with chronic tonsillitis in the Republican Clinical Hospital (Kazan, Russia). The bacterial load was 3.0×10^5 cfu/mL. The fungi load was 2.0×10^3 cfu/mL. Results were recorded every 24 h for 5–7 days. Cultures were incubated at 37 °C. Experiment was repeated three times. Dilutions of compounds were prepared immediately in nutrient media; DMSO (5 % vol.) was added for better solubility so that test strains were not inhibited at this concentration. The minimum inhibitory concentration (MIC) was defined as the minimum concentration of a compound that inhibits the growth of corresponding test microorganism. The growths of bacteria as well as the absence of growth due to the bacteriostatic action of compounds were recorded. To determine minimal bactericidal concentration (MBC), an aliquot of bacterial culture was transferred onto Mueller-Hinton agar or Sabouradu agar in a 10 cm Petri dish and incubated for 24 h at 37 °C. MBC was the minimal concentration at which bacterial colonies were not detected indicating that the bacteria were killed with an efficiency of > 99.9 % [58].

2.11. Hemolytic activity

Hemolytic activity of test compounds was estimated by comparing the optical density of a solution containing the test compound with that of blood at 100 % hemolysis. The experiments were carried out as described earlier [17].

2.12. Cell toxicity assay (MTT-test)

The toxic effect on cells was determined using the colorimetric method of cell proliferation MTT (Thiazolyl Blue Tetrazolium Bromide, Sigma). For this, 10 μL of MTT reagent in Hank's balanced salt solution (HBSS) (final concentration 0.5 mg/mL) was added to each well. The plates were incubated at 37 °C for 2–3 h in an atmosphere humidified with CO_2 (5 % vol.). Absorbance was recorded at 540 nm using an Invitrologic microplate reader (Russia). Experiments for all compounds were repeated three times. The Chang liver cell line (Human liver cells) from the Gamaleya Research Institute of Epidemiology and Microbiology (Moscow, Russia) were used in the experiments. The cells were cultured on standard nutrient medium "Igla" produced by M.P. Chumakov Moscow Institute of Poliomyelitis and Viral Encephalitis with the addition fetal calf serum (10 % vol.) and nonessential amino acids (1 % vol.).

The cells were sown on a 96-well panel from Eppendorf at a concentration of 5×10^3 cells per well in a volume of 100 μL of medium and cultured in a CO_2 incubator at 37 °C. In 48 h after planting the cells, the culture medium was taken into the wells, and 100 μL of solutions of studied drug at specified dilutions were added into the wells. Dilutions of compounds were prepared directly in growth medium supplemented with DMSO (5 % vol.) to improve solubility. The cytotoxic effect of test compounds was determined at concentrations 0.1–100 μM. Calculation of IC_{50}, the concentration of the drug causing 50 % inhibition of cell growth, was performed using the program: MLA- "Quest Graph ™ IC50 Calculator." AAT Bioquest, Inc, June 25, 2022, https://www.aatbio.com/tools/ic50-calculator.

2.13. Anticoagulant and antiaggregation activities in vitro

In vitro experiments were performed using the blood of healthy male donors aged 18–24 years (total 54 donors). The study was approved by the Ethics Committee of Federal State Budgetary Educational Institution of Higher Education at the Bashkir State Medical University of the Ministry of Health of Russian Federation (No.2 dated 17.10.2012). Informed consent was obtained from all participants before blood sampling. The blood was collected from the cubital vein using the system of vacuum blood collection BD Vacutainer® (Becton, Dickinson and Company, USA). A 3.8 % sodium citrate solution in 9:1 ratio was used as a venous blood stabilizer. The study of the effect on platelet aggregation was performed using the Born method [59] using the aggregometer «AT-02» (SPC Medtech, Russia). The assessment of antiplatelet activity of the studied compounds and reference preparations was started with the final concentration of 2×10^{-3} mol/L. Adenosine diphosphate (ADP; 20 μg/mL) and collagen (5 mg/mL) manufactured by Tehnologia-Standart Company, Russia, were used as inducers of aggregation. The study on the anticoagulant activity was performed by standard recognised clotting tests using the optical two-channel automatic analyzer of blood coagulation Solar CGL 2110 (CJSC SOLAR, Belarus). The following parameters were studied: activated partial thromboplastin time (APTT), prothrombin time (PT) and fibrinogen concentrations according to the Clauss method. Determination of anticoagulant activity of studied compounds and reference preparation was performed at concentration of 5×10^{-4} g/mL, using reagents manufactured by Tehnologia-

Standart Company (Barnaul, Russia). Results were processed using the statistical package Statistica 10.0 (StatSoft Inc, USA). The Shapiro-Wilks test was used to check the normality of actual data distribution. The distribution of obtained data differed from the normal one; therefore, for statistical analysis, non-parametric methods were used. The data were presented as medians and 25 and 75 percentiles. Analysis of variance was conducted using the Kruskal-Wallis test. A p value of 0.05 was considered statistical significant.

3. Results and discussion

3.1. Synthesis of amphiphilic isatin derivatives containing an ammonium moiety (Dabco-Is-n)

The synthetic route to Dabco-Is-n quaternary ammonium salts is a two-step one. At the first stage, in accordance with the described procedure [56], monocationic hydrazide **2** was synthesized by the quaternization reaction of 1,4-diazabicyclo[2.2.2] octane. Acylhydrazones **3a-g** were obtained in high yields using acid-catalyzed condensation reaction of DABCO-hydrazide **2** with the corresponding isatins **1a-g** (Scheme 1). The convenience of this approach lies in the fact that the reaction products are isolated in pure form by simple filtration of the cooled reaction masses.

The structures of products were established from elemental and spectroscopic analyses, including IR, ^{1}H NMR, ^{13}C NMR (Figs. S1-S16).

Thus, in the ^{1}H NMR spectrum of Dabco-Is-12 (**3d**) the upfield characteristic signal of the methyl group appears as a triplet with δ_H 0.79 ppm, as well as signals of the CH_2 group of the alkyl chain as multiplets, and the signals of the protons of the methylene group, directly bonded to the oxindole nitrogen atom appear as a triplet at 3.65 ppm. The signal of the protons of the methylene groups of the DABCO fragment at the quaternary nitrogen atom appears at δ_H 4.18 ppm, while the resonance of the protons of the methylene groups bonded with the uncharged nitrogen atom appears at δ_H 3.46 ppm. The proton signal of the CH_2 group located between the ammonium center and the carbonyl group of the hydrazone fragment appears as a broadened singlet at 5.17 ppm. The region of low fields of the ^{1}H NMR spectrum contains signals of aromatic protons and a broadened low-intensity signal at 12.75 ppm, attributed to the proton of the NH group.

In the IR spectra of compounds **3a-g**, the absorption bands corresponding to the vibrations of the N—H bonds ($\nu \sim 3400$ cm^{-1}), C=O (ν = 1719–1709 cm^{-1}), C=C (ν = 1612–1617 cm^{-1}) and C=N (ν = 1451–1468 cm^{-1}) are the most significant.

3.2. Self-assembly and solubilization properties of Dabco-Is-n

The self-assembly of Dabco-Is-n was studied by tensiometry, conductometry, spectrophotometry and dynamic light scattering. Dabco-Is-n solutions in water were transparent, suggesting that their Krafft points are below 20 °C. Experimentally found Krafft point values are below 25 °C. Surface tension isotherms of all compounds at the air–water interface as a function of their concentration are shown in Fig. 1.

The adsorption characteristics were obtained using tensiometric and conductometric (Fig. 1) data. The values of surface excess (Γ_{max}), surface area per molecule (A_{min}), standard free energy of micellization per mole of monomer unit (ΔG_m) and standard free energy of interfacial adsorption at the air/saturated monolayer interface (ΔG_{ad}) were calculated using equations (2)-(7) [60–62].

$$\Gamma_{\max} = -\frac{1}{2.3mRT}\lim_{C\to cmc}(d\pi/d\log C) \quad (2)$$

where the constant m = 2 as for monomeric ionic surfactant.

$$A_{min} = 10^{18}/(N_A\Gamma_{max}) \quad (3)$$

where N_A is the Avogadro number (6.02 × 10^{23} mol^{-1}).

The ability of a surfactant to reduce the surface tension by 20 mN m^{-1} (pC_{20}) is:

$$pC_{20} = -logC_{20} \quad (4)$$

where C_{20} is the molar concentration required to reduce the surface tension by 20 mN m^{-1}.

$$\Delta G_{ad} = \Delta G_m - (\pi_{CMC}/\Gamma_{max}) \quad (5)$$

$$\Delta G_m = RT(1+\beta)ln(CMC) \quad (6)$$

Here, β is the counterion binding degree calculated via Eq. (7), i.e. from the slope ratio of specific conductivity vs concentration plots (Fig. 2) presented in Table 1.

$$\beta = 1 - [d\chi/dC]_{C>CMC}/[d\chi/dC]_{C<CMC} \quad (7)$$

The adsorption characteristics and critical micelle concentration (CMC) values are presented in Table 1. CMC values determined by different methods tensiometry, conductometry (Fig. 1) and spectrophotometry (deviations from Beer-Lambert, Fig. S17) are very close.

CMC values of Dabco-Is-n homologs with n = 10, 12, 14 are>10 times lower than for Dabco-n surfactants (Fig. 2A). CMC of Dabco-Is-12 is 2 times lower than isatin derivatives containing trimethylammonium moiety (Is-n, where n = 12). As we noted in our previous work, the presence of isatin skeleton in the structure of cationic amphiphile promotes the easiest self-assembly process.

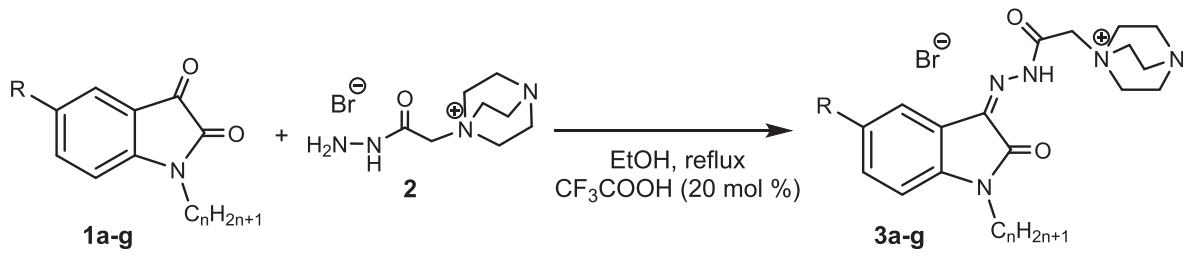

R = H, n = 10 (a); R = CH_3, n = 10 (b); R = Cl, n = 10 (c); R = H, n = 12 (d);
R = H, n = 14 (e); R = H, n = 16 (f); R = H, n = 18 (g)

Scheme 1. Synthesis of amphiphilic isatin derivatives Dabco-Is-n containing a quaternary ammonium moiety, where n = 10, R = H (Dabco-Is-10), CH_3 (Dabco-Is-CH_3-10), Cl (Dabco-Is-Cl-10); R = H, n = 12 (Dabco-Is-12), 14 (Dabco-Is-14), 16 (Dabco-Is-16), 18 (Dabco-Is-18).

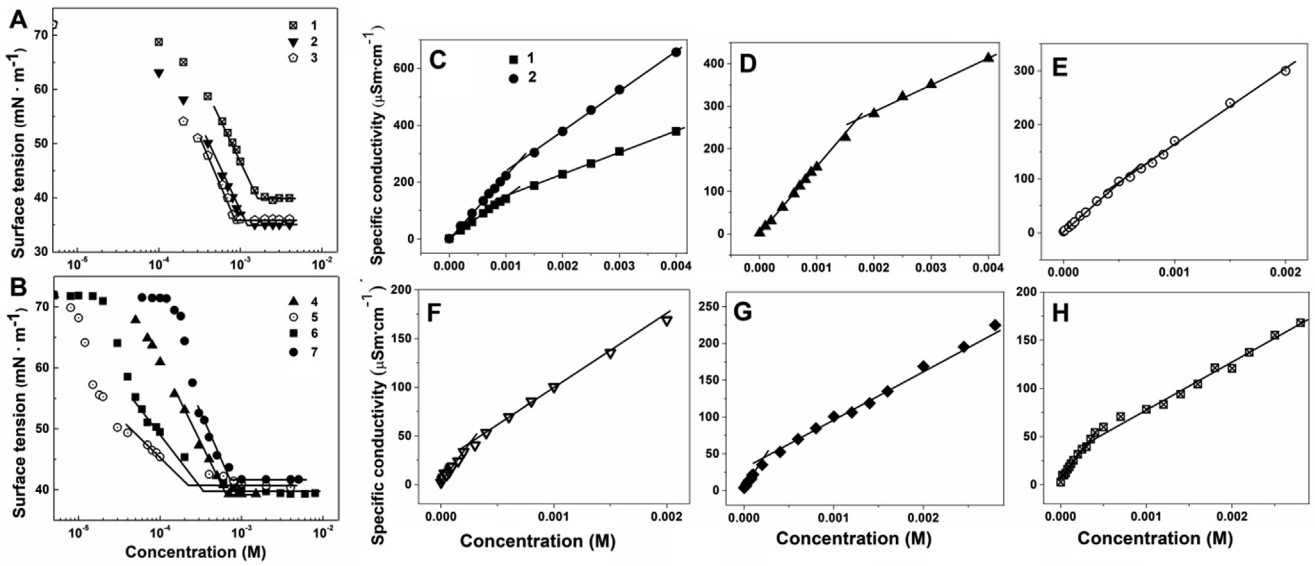

Fig. 1. Surface tension isotherms (A, B) of Dabco-Is-10 (1), Dabco-Is-Cl-10 (2), Dabco-Is-CH_3-10 (3) and Dabco-Is-n, where n = 12 (4), 14 (5), 16 (6), 18 (7) and specific conductivity Dabco-Is-R-10 (C), where R = Cl (1), CH_3 (2) and Dabco-Is-n, where n = 10 (D), 12 (E), 14 (F), 16 (G), 18 (H), 25 °C.

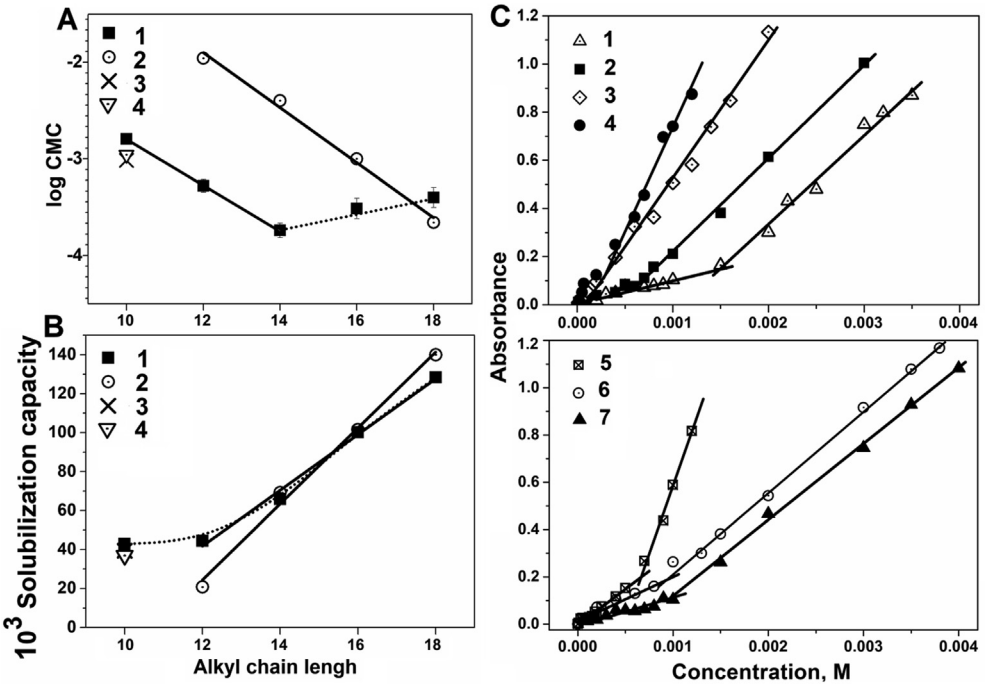

Fig. 2. Effect of the alkyl chain length on CMC (A), solubilization capacity (B) for Dabco-Is-n (1), Dabco-n (2), Dabco-Is-CH_3-10 (3), Dabco-Is-Cl-10 (4) and absorbance of Sudan I (C) in solutions of Dabco-Is-n, where n = 10 (1), 12 (2), 14 (3), 16 (4), 18 (5) and Dabco-Is-CH_3-10 (6), Dabco-Is-Cl-10 (7), L = 0.1 cm, 25 °C, λ = 485 nm.

Namely, cationic amphiphiles with isatin fragment have the possibility of hydrogen bond formation and π-π-stacking interactions unlike cationic surfactants [45]. The energy needed for formation of Dabco-Is-n self-assemblies (energy required to overcome the repulsion involved in bringing two charged quaternary ammonium groups close together) may come from the energy released upon disruption of hydrogen bonds and π-π-stacking interactions. In our study the presence of DABCO significantly altered the CMC of these new ammonium amphiphiles as compared to the properties of typical cationic surfactants. It is a rather unique case when the presence the two fragments (DABCO and an isatin skeleton) in a molecule synergistically improves the self-assembly process. Thus, Dabco-Is-n shows no typical mechanism of self-assembly micelle formation compared to monomeric ionic surfactants.

It is known that log CMC typical ionic surfactants decreases linearly with the increase in n, according to the empirical Klevens equation [63]: log CMC = A – Bn_C.

The linearity of plots following the Klevens equation can be described as:

log CMC = -0.44–0.236n_c, r = 0.999 (for Dabco-Is-n, n = 10, 12, 14).

The slope is 0.236, a value smaller than for Dabco-n (where n = 12, 14, 16, 18), which is 0.284 [49] and typical ionic surfactants, which is 0.28–0.30 [64,65]. This suggests that Dabco-Is-n are less

Table 1
CMC values determined by tensiometry, conductometry and spectrophotometry, the counterion binding degree (β).

Cationic amphiphiles	CMC × 10^3 (M)			β	π_{cmc} (mN/m)
	Tensiometry	Conducto-metry	Spectro-photometry		
Dabco-Is-10	1.6	1.7	1.5	0.59	39.8
Dabco-Is-CH_3-10	0.9	1	0.9	0.54	36.02
Dabco-Is-Cl-10	1.1	1.2	1.1	0.36	35.06
Dabco-Is-12	0.65	0.45	0.44	0.24	39.3
Dabco-Is-14	0.2	0.2	0.15	0.47	40.76
Dabco-Is-16	0.35	0.2	0.27	0.64	44.66
Dabco-Is-18	0.6	0.4	0.2	0.59	41.7
Is-Q-16[a]	0.46	0.3	0.1	0.17	28.2
Dabco-16[b]	1	1	–	0.77	28.3
CTAB[b]	1	0.8	0.8	0.77	33.3

[a] [45].
[b] [49].

hydrophobic than typical ammonium surfactants. In addition, the long chain Dabco-Is-16 and Dabco-Is-18 show deviation from linearity compared to monomeric ionic surfactants.

The lowest CMC, adsorption efficiency (pC_{20}), Γ_{max} and minimum energy of adsorption (ΔG_{ad}) and micellization (ΔG_m) are observed for Dabco-Is-14 (Table 1, 2). Dabco-Is-14 has the maximum of surface area per molecule on water–air surface. This indicates that the Dabco-Is-n molecules with increasing chain length from 10 to 14 pack bulky at the water–air surface. Tightly packaging and increasing adsorption at the water–air surface by increasing the chain length from 14 to 18 are observed. The same deviation from linearity in log CMC and adsorption characteristics was shown for the long-chain gemini surfactants [66–69].

This aberrant behavior can be explained by the formation of submicellar structures and premicellar aggregates. That enhances its aggregation propensity. This single-chain pyridinium surfactant forms lamellar aggregates [70]. Some single-chain pyridinium surfactant also forms vesicular aggregate [71]. In our work, the formation of lamellar hexagonal packing for Dabco-Is-16 was observed by using polarized optical microscopy (Fig. S18). Dabco-Is-16 can form «amphiphilic π-π-pairs» like «gemini surfactants», producing a premicellar associates or dimers by hydrogen bonds and π-π-stacking interactions and then symmetrical membrane or vesicles. Formation of symmetrical membrane can be easily realized with increasing derivative chain length [72]. The DLS method confirms that Dabco-Is-n organized nanoparticles with a size about 100 nm or more (Table S1, Fig. S19). Zeta potential values of Dabco-Is-n are positive about + 50 mV.

Solubilization properties of Dabco-Is-n were analyzed toward solubilization of the hydrophobic dye (Sudan I) as a model hydrophobic drug. The absorption spectra of Sudan I (λ_{max} = 485 nm) in Dabco-Is-n solutions with increasing their concentration are presented in Fig. S20. Usually cationic surfactants dissolve hydrophobic compounds inside the micellar core [52]. The drug solubility can be improved by formation of electrostatic and dipole interactions between surfactants and drugs. Solubilization capacity of Dabco-Is-n (the number of moles of dye solubilized per mole of Dabco-Is-n) presented in Fig. 2B. It was determined by the slope of the growth of Sudan I absorbance (at λ_{max} = 485 nm) with increasing of Dabco-Is-n concentration (Fig. 2C). Solubility of dyes linearly increases with alkyl chain length of Dabco-Is-n (from n = 12 to n = 18) and follows the relation: S = -0.12995 + 0.01431n, r = 0.996.

The solubilization capacity of Dabco-Is-n with increasing long chains reaches the solubilization properties of cationic hexadecyl classical analogues (Dabco-n and CTAB) and long chain geminal surfactants [73]. In the case of dodecyl analog Dabco-Is-12, the solubilization capacity is 2 times higher than for Dabco-12 [52]. All decyl derivatives Dabco-Is show high solubilizing activity.

Due to differences between Dabco-Is-12 and Dabco-Is-16 in self-assembly and solubilization properties, their FTIR spectra in the absence and presence Sudan I and poorly water-soluble drugs (niclosamide and piperine) were investigated. Niclosamide and piperine are under our consideration for their high potential to counter various viral infections and resistant bacteria [74,75]. The transmittance signals were observed at 1467 and 1467 cm^{-1} due to $\upsilon_{C=C}$, 1675 and 1677 cm^{-1} due to $\upsilon_{C=O}$, 1706 and 1709 due to $\upsilon_{C=O}$ (cycle) for Dabco-Is-12 (Fig. 3A line 1) and Dabco-Is-16 (Fig. 3D, line 1), respectively in KBr.

In case of Dabco-Is-12 the transmittance signals of carbonyl shifted from 1675 cm^{-1} to 1681 cm^{-1} and 1686 cm^{-1} in the presence a Sudan I and niclosamide and piperine, respectively. The transmittance signals of carbonyl (cycle) moved from 1706 cm^{-1} to 1709, 1711 and 1714 cm^{-1}, respectively. Transmittance signals of carbonyl for Dabco-Is-16 shifted in the shortwave direction from

Table 2
Values of surface excess (Γ_{max}), surface area per surfactant molecule (A_{min}), standard free energy of micellization per mole of monomer unit (ΔG_m) and the standard free energy of interfacial adsorption at the air/saturated monolayer interface (ΔG_{ad}).

Cationic amphiphiles	pC_{20}	Γ_{max} × 10^6 (mol m^{-2})	A_{min} (nm^2)	ΔG_{ad} (kJ mol^{-1})	ΔG_m (kJ mol^{-1})
Dabco-Is-10	3.17	2.81	0.59	−42.1	−30.67
Dabco-Is-CH_3-10	3.52	3.18	0.52	−43.4	−32.07
Dabco-Is-Cl-10	3.45	3.01	0.55	−39.9	−27.67
Dabco-Is-12	3.66	1.95	0.85	−42.94	−26.29
Dabco-Is-14	4.5	1.1	1.52	−63.4	−34.9
Dabco-Is-16	4.17	1.58	1.05	−56.76	−36.27
Dabco-Is-18	3.47	3.18	0.52	−42.36	−32.85
Is-Q-16[a]	3.66	2.4	0.68	−36.25	−24.7
Dabco-16[b]	3.3	2.37	0.7	−45.0	−33.0
CTAB[b]	3.54	3.10	0.53	−37.5	−30.6

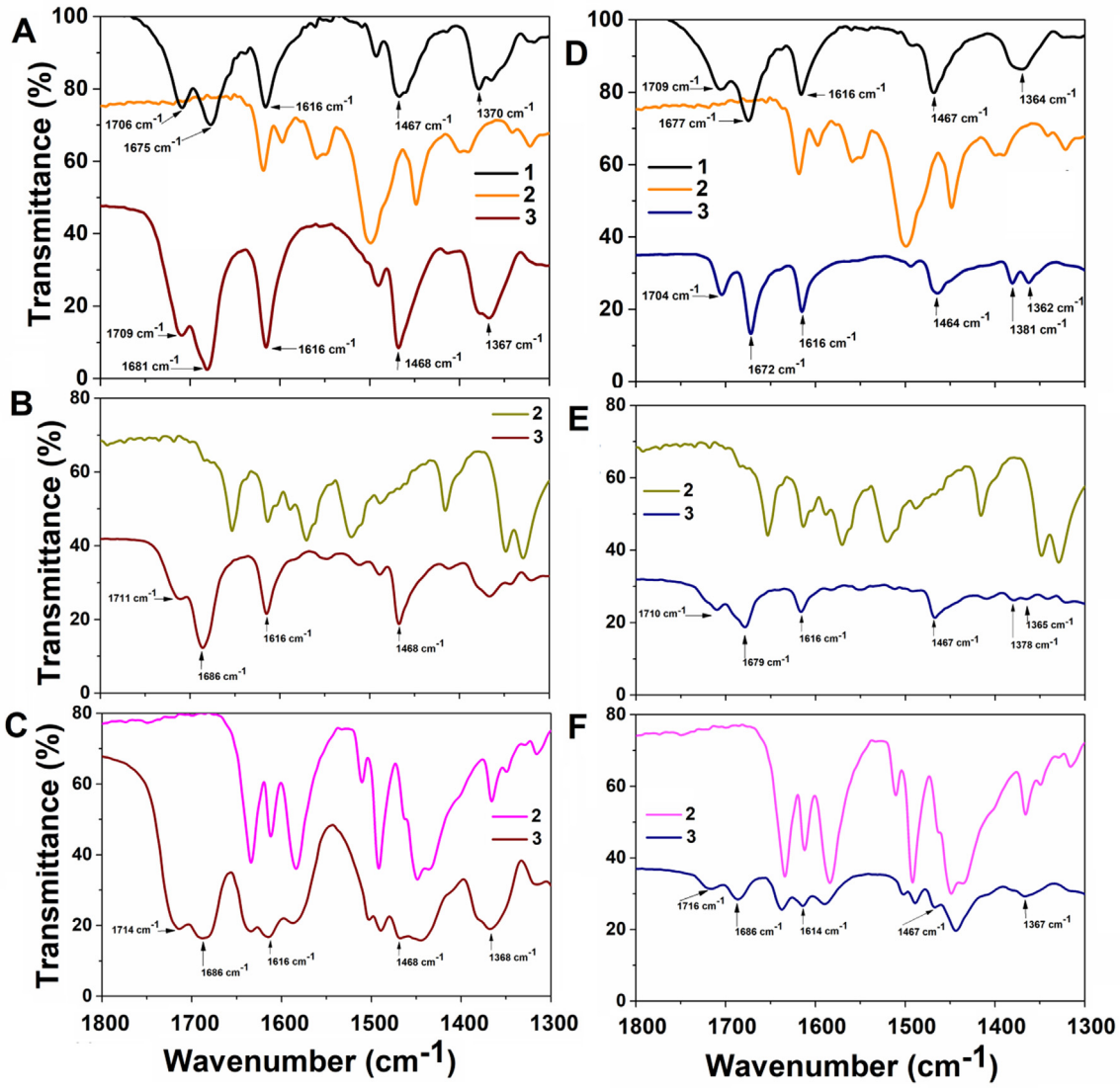

Fig. 3. FTIR spectra of Dabco-Is-12 (A-C) and Dabco-Is-16 (D-F) in absence (A, D, line 1) and presence Sudan I (A, D, line 3), drugs Niclosamide (B, E, line 3), Piperine (C, F, line 3) and Sudan I (A,D, line 2), Niclosamide (B, E, line 2), Piperine (C, F, line 2) in KBr pallet, 25 °C.

1677 cm^{-1} to 1672 cm^{-1} in the presence as a Sudan I and weakly moved in the presence niclosamide from 1677 cm^{-1} to 1679 cm^{-1}. It is known that strong hydrogen-bond is capable of perturbing C═O, causing the greater shift of carbonyl signals. The lower CMC values (more than an order of magnitude) for Dabco-Is-n with n = 10, 12, and 14 also confirm this assumption. The hydrogen-bond interactions affect the improvement of solubility of poorly water-soluble dye and drugs for Dabco-Is-n with n = 10, 12 compared to classical ammonium surfactants.

3.3. Antibacterial and antifungal activity of DABCO-Is-n

The *in vitro* antibacterial and antifungal activities of DABCO-Is-n were evaluated for a wide spectrum of pathogenic bacteria as indicated in Materials and Methods. Dabco-Is-12 is the most perspective compound with high activity and potency against pathogenic representatives of Gram-positive Bacteria *Staphylococcus aureus ATCC 209p*, *Enterococcus faecalis ATCC 29212*, methicillin-resistant *Staphylococcus aureus MRSA-1* and *MRSA-2* and against fungus *Candida albicans NCTC 885–653* (Table 3). The MRSA-1 strain was resistant to fluoroquinolone antibiotic ciprofloxacin and β-lactam antibiotic amoxicillin. The MRSA-2 strain was resistant only to amoxicillin. In the test against Gram-positive bacteria *Sa* and *Ef* Dabco-Is-12 exhibited 7 and 3.5 times, respectively, higher bacterial activity than that of Chloramphenicol. Dabco-Is-12 showed high activity against *MRSA-1* and *MRSA-2* (MIC = 3.5 and 7.0 μM, respectively). This value is>70 times higher (against *MRSA-1*) and comparable (against *MRSA-2)* to activity of the antibiotic Norfloxacin [76,77]. It should be noted that Dabco-Is-n are not toxic. Thus, evaluated IC_{50} are ≥ 100 μM (Table 3) and HC_{50} is much higher than HC_{50} of antibiotics against gram-positive bacteria Gramicidin (9.4 ± 0.7 μM).

Effect of alkyl chain length on CMC, the HC_{50} of human erythrocytes, MIC against *S. aureus* is presented in Fig. 4A.

The MIC and HC_{50} of Dabco-Is-n slightly decrease with increasing alkyl chain length (Fig. 4A). This profile is not linear as a dependence of the CMC. Dabco-Is-16 and Dabco-Is-18 are inactive against bacterial strains tested. This behavior is very different from ammonium Dabco-n surfactant (Fig. 4A, insert). Thus, MIC values of Dabco-Is-n are lower than CMC of Dabco-Is-n in one order of magnitude. These values are very close to CMC in biological environment [78]. That is, self-assemblies of Dabco-Is-n are responsible factor for antimicrobial activity. Unlike Dabco-n where antimicrobial activity is associated with the lipophilicity of single Dabco-n molecule. Dabco-Is-n are bactericides and fungicides (MBC/MIC is les then 4) unlike Dabco-n surfactants [51], which display only

Table 3
Antimicrobial activities (minimum inhibitory concentration (MIC) and minimum bactericidal and fungicidal concentration (MBC) μM and hemolytic (HC_{50}, μM) and cytotoxic (IC_{50}, μM) effect of compounds **3a-g** on erythrocytes and liver cells (Chang liver).

Compounds	MIC (μM)				MBC (μM)				HC_{50} (μM)	IC_{50} (μM)
	Sa	*Bc*	*Ef*	*Ca*	*Sa*	*Bc*	*Ef*	*Ca*		
Dabco-Is-CH_3-10	28.5 ± 2.4	56.9 ± 4.4	>500	>500	56.9 ± 4.3	228 ± 19	>500	>500	>100	100
Dabco-Is-Cl-10	27.5 ± 2.2	54.9 ± 4.4	>500	>500	54.9 ± 4.5	220 ± 18	>500	>500	60.2	79.0
Dabco-Is-10	58.5 ± 4.6	58.5 ± 4.7	>500	>500	117 ± 9.1	58.5 ± 4.5	>500	>500	74.2	99.2
Dabco-Is-12	13.9 ± 1.1	>500	27.7 ± 2.3	27.7 ± 2.2	13.9 ± 1.2	>500	27.7 ± 2.2	27.7 ± 2.1	98.4	>100
Dabco-Is-14	26.5 ± 2.1	>500	26.5 ± 2.0	212 ± 16	106 ± 8.2	>500	52.9 ± 4.1	212 ± 17	31.8	>100
Dabco-12[a]	34.6	86.6	–	346	>500	>500	–	>500	>250	–
Dabco-14[a]	7.95	20.0	–	160.5	>500	>500	–	>500	80.1	–
Is-12[b]	16.7 ± 1	134.3	–	269	33.5	269	–	>500	107	–
Is-14[b]	>500	>500	–	36.1	>500	>500	–	144.6	131	–
Chloramphenicol	96.7 ± 7.5	193.5 ± 15.3	96.7 ± 7.6	–	–	–	–	–	–	–

[a] [51].
[b] [45].

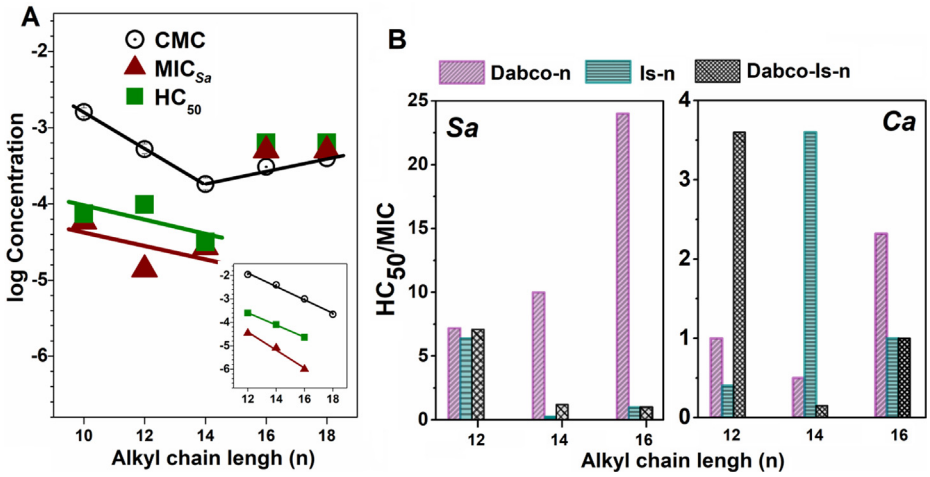

Fig. 4. Effect of the alkyl chain length (n) on MIC against *S. aureus*, CMC and the HC_{50} of human erythrocytes Dabco-Is-n and Dabco-n (insert) (A) Antimicrobial selectivity index (HC_{50}/MIC) against *S. aureus* and *Ca* (B).

bacteriostatic and fungistatic properties. Thus the combination of isatin and ammonium fragments in one molecule helps to improve bactericidal properties.

Therapeutic or antimicrobial selectivity index (HC_{50}/MIC) is used to assess the selectivity of antimicrobial agents. The effect of structural fragments (Dabco ammonium and isatin fragments), as well as their combination and variation with the alkyl chain length for optimization of antibacterial activity are considered in Fig. 4B. Alkyl chain length of QACs has a significant effect on the selectivity index against Gram-positive bacteria (*S. aureus*). For example, the selectivity index increases in the case of Dabco-n and rapidly decreases for Dabco-Is-n and Is-n. This behavior is likely associated to the unlike traditional micelle formation mechanism of Dabco-Is-n or to vesicular structures and lyotropic mesophases of long chain Dabco-Is-n. The opposite behavior is observed against Gram-negative bacteria. Less lipophilic Dabco-Is-n showed more selectivity index against *Candida albicans.* Likely this is attributed to the difference in *Ca* cell outer membrane. Disrupting the integrity of outer membrane by the electrostatic interaction between cationic Dabco-Is-n self-assemblies and the anionic surface of *Ca* is accompanied by the non-covalent (hydrogen bonding) bonds between of isatin scaffold and lipopolysaccharides of *Ca* (Scheme 2).

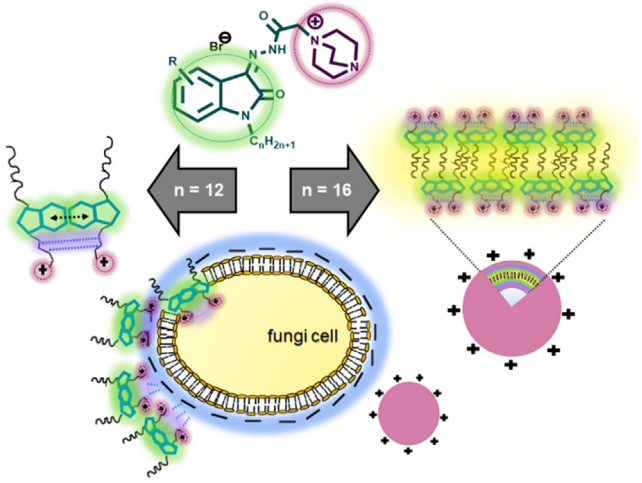

Scheme 2. Dabco-Is-n self-assemblies' formation and their possible antibacterial action.

3.4. Anticoagulant and anti-aggregation activities of DABCO-Is-n

According to the results of the studies, it was found that all compounds cause hypocoagulation, increasing the median values of APTT by 1.1–8.1 % compared with the control, without affecting the concentration of fibrinogen and prothrombin time. At the same time, Dabco-Is-12, Dabco-Is-14 and Dabco-Is-16 exhibit anti-aggregation activity at the level of acetylsalicylic acid (ASA) in terms of maximum amplitude (Table 4) and statistically signifi-

Table 4
Influence of compounds and reference drugs acetylsalicylic acid (ASA) and heparin sodium (HS) on the indicators of platelet aggregation and coagulation element of hemostasis, Me (0.25–0.75).

Compound	Latent period, % of control	Maximum amplitude, % to control	Aggregation rate, % to control	Time to reach maximum amplitude, % of control	APTT, % to control
Dabco-Is-10	+12.4 (11.6–15.7)$^{*, \#}$	−19.6 (14.3–21.5)$^{*,\#}$	+9.3 (7.3–10.4)$^{*, \#}$	−8.7 (7.4–10.8)$^{*, \#}$	+7.1 (6.3–9.5)§
Dabco-Is-CH_3-10	−11.2 (8.9–14.3)$^{*, \#}$	−3.5 (2.7–6.4)$^{\#}$	−12.9 (11.5–14.3)*	−14.5 (12.7–19.3)$^{**,\#}$	+8.1 (7.3–10.2)§
Dabco-Is-Cl-10	−4.1 (3.7–5.9)	−7.4 (6.5–10.3)$^{*, \#}$	−11.4 (8.6–12.9)*	+32.1 (30.1–37.4)$^{*,\#}$	+3.4 (2.7–4.5)§
Dabco-Is-12	+12.7 (11.5–17.6)$^{*, \#}$	−13.1 (10.4–15.9)*	−11.5 (7.9–12.8)*	−24.5 (22.8–27.9)$^{*, \#}$	+3.7 (2.8–4.5)§
Dabco-Is-14	+11.8 (10.7–15.9)$^{*, \#}$	−10.3 (7.2–13.6)*	−14.8 (11.1–15.6)*	−14.6 (12.3–17.5)$^{*, \#}$	+7.2 (5.3–9.1)§
Dabco-Is-16	+10.5 (8.9–14.5)$^{*, \#}$	−14.5 (12.7–16.9)*	−21.7 (16.5–23.9)$^{**, \#}$	+7.2 (6.1–8.3)$^{*, \#}$	+1.9 (1.2–2.7)§
Dabco-Is-18	+3.5 (3.2–5.4)	−7.1 (6.9–9.1)$^{*, \#}$	+5.3 (6.2–8.7)$^{*, \#}$	−12.9 (11.5–16.7)$^{*, \#}$	+6.8 (5.7–8.3)§
ASA	−2.1 (1.1–2.6)	−13.7 (10.8–16.4)*	−10.5 (7.6–12.3)*	+10.5 (8.7–13.4)*	+1.1 (0.5–1.9)§
HS	–	–	–	–	+20.3 (19.7–21.4)**

$^{*}p \leq 0.05$, $^{**}p \leq 0.001$ - compared to control; $\#p \leq 0.05$, $\#\#p \leq 0.001$ - compared to ASA; $^{\S}p \leq 0.05$ - compared to HS.

cantly increase the lag-period (platelet release response) and more effective than acetylsalicylic acid reduce the rate of platelet aggregation.

A similar effect is shown by Dabco-Is-18, which is slightly inferior to the reference drug in terms of maximum amplitude. The most active compound is Dabco-Is-10, which surpasses ASA by 31.2 % in terms of the maximum amplitude. Thus, all investigated compounds do not have a significant thrombogenic potential and slightly change the overall coagulation potential towards hypocoagulation.

4. Conclusions

New quaternary ammonium compounds based on the isatin skeleton in combination with DABCO fragment (Dabco-Is-n, where n = 10, 12, 14, 16, 18) were synthesized and characterized by FT-IR and NMR spectra. The influence structure fragments (chain length and the nature of substituent in aromatic fragment) on adsorption, self-assembled and solubilization properties, antimicrobial activity, toxicity and blood factors was revealed. The CMC of Dabco-Is-n is>10 times lower than CMC of Dabco-surfactant and classical analogs. Low toxic, low hemolytic and highly biocompatible (IC_{50} and HC_{50} are $\geq$ 100 μM, negligible thrombogenic coagulation potential) Dabco-Is-12 with high biological activity against methicillin-resistant bacterial strains *MRSA-1* and *MRSA-2* (MIC = 3.5 and 7.0 μM, respectively) and high solubilization capacity toward hydrophobic dye (Sudan I) and it's implementation for hydrogen-bonds with drugs (niclosamide and piperine) and good selectivity index toward fungi *C. albicans* has a high potential for medical applications.

Data availability

No data was used for the research described in the article.

Declaration of Competing Interest

The authors declare that they have no known competing financial interests or personal relationships that could have appeared to influence the work reported in this paper.

Acknowledgements

T.N.P., Z.M.S, A.E.V, A.D.V., A.V.B., V.F.M. acknowledge the financial support received from the government assignment for FRC Kazan Scientific Center of Russian Academy of Sciences. The measurements have been carried out using the equipment of Distributed Spectral-Analytical Center of Shared Facilities for Study of Structure, Composition and Properties of Substances and Materials of FRC Kazan Scientific Center of RAS. Study of antiplatelet and antiaggregation activities was performed according to the cooperation agreement between the Kazan Scientific Center (Russian Academy of Sciences) and Bashkir State Medical University (Ministry of Health of the Russian Federation).

References

[1] N. Nikfarjam, M. Ghomi, T. Agarwal, M. Hassanpour, E. Sharifi, D. Khorsandi, M. Ali Khan, F. Rossi, A. Rossetti, E. Nazarzadeh Zare, N. Rabiee, D. Afshar, M. Vosough, T. Kumar Maiti, V. Mattoli, E. Lichtfouse, F.R. Tay, P. Makvandi, 31 (2021) 2104148.
[2] A.M. Curreri, S. Mitragotri, E.E.L. Tanner, 8 (2021) 2004819.
[3] M.R. Salton, J. Gen. Microbiol. 5 (1951) 391.
[4] M.R. Salton, J. General Physiol. 52 (1968) 227Suppl.
[5] V.D. Sharma, E.O. Aifuwa, P.A. Heiney, M.A. Ilies, Biomaterials 34 (2013) 6906.
[6] X. Xie, W. Cong, F. Zhao, H. Li, W. Xin, G. Hou, C. Wang, Journal of enzyme inhibition and medicinal chemistry 33 (2018) 98.
[7] L. Zheng, J. Li, M. Yu, W. Jia, S. Duan, D. Cao, X. Ding, B. Yu, X. Zhang, F.J. Xu, J. Am. Chem. Soc. 142 (2020) 20257.
[8] J. Hoque, M.M. Konai, S. Samaddar, S. Gonuguntala, G.B. Manjunath, C. Ghosh, J. Haldar, Chem. Commun. 51 (2015) 13670.
[9] A.R. Ahmady, P. Hosseinzadeh, A. Solouk, S. Akbari, A.M. Szulc, B.E. Brycki, Adv. Colloid Interface Sci. 299 (2022) 102581.
[10] S. Zhang, S. Ding, J. Yu, X. Chen, Q. Lei, W. Fang, Langmuir 31 (2015) 12161.
[11] R.A. Allen, M.C. Jennings, M.A. Mitchell, S.E. Al-Khalifa, W.M. Wuest, K.P.C. Minbiole, Bioorg. Med. Chem. Lett. 27 (2017) 2107.
[12] L. Pérez, R. Pons, F.F. Oliveira de Sousa, M.d.C. Morán, A. Ramos da Silva, A. Pinazo, Journal of Molecular Liquids 339 (2021) 116819.
[13] D.R. Perinelli, D. Petrelli, L.A. Vitali, D. Vllasaliu, M. Cespi, G. Giorgioni, E. Elmowafy, G. Bonacucina, G.F. Palmieri, J. Mol. Liq. 283 (2019) 249.
[14] A. Pinazo, M.A. Manresa, A.M. Marques, M. Bustelo, M.J. Espuny, L. Pérez, Adv. Colloid Interface Sci. 228 (2016) 17.
[15] O.V. Andreeva, B.F. Garifullin, V.V. Zarubaev, A.V. Slita, I.L. Yesaulkova, A.S. Volobueva, M.G. Belenok, M.A. Man'kova, L.F. Saifina, M.M. Shulaeva, A.D. Voloshina, A.P. Lyubina, V.E. Semenov, V.E. Kataev, Molecules (Basel, Switzerland) 26 (2021).
[16] V.E. Kataev, B.F. Garifullin, Chem. Heterocycl. Compd. 57 (2021) 326.
[17] A.D. Voloshina, A.S. Sapunova, N.V. Kulik, M.G. Belenok, I.Y. Strobykina, A.P. Lyubina, S.K. Gumerova, V.E. Kataev, Bioorg. Med. Chem. 32 (2021) 115974.
[18] N. Joondan, P. Caumul, G. Jackson, S. Jhaumeer Laulloo, Chem. Phys. Lipids 235 (2021) 105051.
[19] D.K. Kaczmarek, T. Rzemieniecki, D. Gwiazdowska, T. Kleiber, T. Praczyk, J. Pernak, J. Mol. Liq. 327 (2021) 114792.
[20] D.K. Kaczmarek, T. Kleiber, L. Wenping, M. Niemczak, Ł. Chrzanowski, J. Pernak, ACS Sustainable Chem. Eng. 8 (2020) 1591.
[21] J. Pernak, T. Rzemieniecki, T. Klejdysz, F. Qu, R.D. Rogers, ACS Sustainable Chem. Eng. 8 (2020) 9263.
[22] L. Bazina, A. Maravić, L. Krce, B. Soldo, R. Odžak, V.B. Popović, I. Aviani, I. Primožič, M. Šprung, Eur. J. Med. Chem. 163 (2019) 626.
[23] M. Skočibušić, R. Odžak, Z. Štefanić, I. Križić, L. Krišto, O. Jović, T. Hrenar, I. Primožič, D. Jurašin, Colloids and surfaces, B, Biointerfaces 140 (2016) 548.
[24] J. Ma, N. Liu, M. Huang, L. Wang, J. Han, H. Qian, F. Che, J. Mol. Liq. 294 (2019) 111669.
[25] M.D. Joyce, M.C. Jennings, C.N. Santiago, M.H. Fletcher, W.M. Wuest, K.P. Minbiole, The Journal of antibiotics 69 (2016) 344.
[26] F. Martin, T. Grkovic, M.L. Sykes, T. Shelper, V.M. Avery, D. Camp, R.J. Quinn, R. A. Davis, J. Nat. Prod. 74 (2011) 2425.
[27] A.S. Sokolova, C.O. Yarovaya, C.A. Shernyukov, C.E. Pokrovsky, C.A. Pokrovsky, V.A. Lavrinenko, V.V. Zarubaev, T.S. Tretiak, P.M. Anfimov, O.I. Kiselev, A.B. Beklemishev, N.F. Salakhutdinov, Bioorg. Med. Chem. 21 (2013) 6690.
[28] A. Radman Kastelic, R. Odžak, I. Pezdirc, K. Sović, T. Hrenar, A. Čipak Gašparović, M. Skočibušić, I. Primožič, Molecules (Basel, Switzerland) 24 (2019).

[29] D.S. Chauhan, M.A. Quraishi, A. Qurashi, J. Mol. Liq. 326 (2021) 115117.
[30] C. Zhou, Y. Wang, Curr. Opin. Colloid Interface Sci. 45 (2020) 28.
[31] O. Soukup, M. Benkova, R. Dolezal, R. Sleha, D. Malinak, S. Salajkova, A. Markova, M. Hympanova, L. Prchal, L. Ryskova, L. Hobzova, K. Sepčić, N. Gunde-Cimerman, J. Korabecny, D. Jun, V. Bostikova, P. Bostik, J. Marek, Eur. J. Med. Chem. 206 (2020) 112584.
[32] D. Crnčević, L. Krce, L. Mastelić, A. Maravić, B. Soldo, I. Aviani, I. Primožič, R. Odžak, M. Šprung, Bioorg. Chem. 112 (2021) 104938.
[33] C.E. Drakontis, S. Amin, Curr. Opin. Colloid Interface Sci. 48 (2020) 77.
[34] T.R. Bjerk, P. Severino, S. Jain, C. Marques, A.M. Silva, T. Pashirova, E.B. Souto, Bioengineering (Basel, Switzerland) 8 (2021).
[35] H. Guo, Eur. J. Med. Chem. 164 (2019) 678.
[36] C. Melis, R. Meleddu, A. Angeli, S. Distinto, G. Bianco, C. Capasso, F. Cottiglia, R. Angius, C.T. Supuran, E. Maccioni, J. Enzyme Inhib. Med. Chem. 32 (2017) 68.
[37] P. Brandão, C. Marques, A.J. Burke, M. Pineiro, Eur. J. Med. Chem. 211 (2021) 113102.
[38] Y.Z. Zhang, H.Z. Du, H.L. Liu, Q.S. He, Z. Xu, Arch. Pharm. 353 (2020) e1900299.
[39] R.E. Ferraz de Paiva, E.G. Vieira, D. Rodrigues da Silva, C.A. Wegermann, A.M. Costa Ferreira, Front Mol Biosci 7 (2021) 627272.
[40] R. Kumar, P. Takkar, Med. Chem. Res. 30 (2021) 847.
[41] F. Song, Z. Li, Y. Bian, X. Huo, J. Fang, L. Shao, M. Zhou, Arch. Pharm. 353 (2020) e2000143.
[42] I. Shagufta, Ahmad, Eur. J. Med. Chem. 213 (2021) 113157.
[43] K.L. Vine, L. Matesic, J.M. Locke, M. Ranson, D. Skropeta, Anti-Cancer Agents Med. Chem. 9 (2009) 397.
[44] K.L. Vine, L. Matesic, J.M. Locke, D. Skropeta, Adv. Anticancer Agents Med. Chem. 2 (2013) 254.
[45] T.N. Pashirova, A.V. Bogdanov, I.F. Zaripova, E.A. Burilova, A.E. Vandyukov, A.S. Sapunova, I.I. Vandyukova, A.D. Voloshina, V.F. Mironov, L.Y. Zakharova, J. Mol. Liq. 290 (2019) 111220.
[46] R.C. Kontos, S.A. Schallenhammer, B.S. Bentley, K.R. Morrison, J.A. Feliciano, J.A. Tasca, A.R. Kaplan, M.W. Bezpalko, W.S. Kassel, W.M. Wuest, K.P.C. Minbiole, ChemMedChem 14 (2019) 83.
[47] A.J. Leitgeb, J.A. Feliciano, H.A. Sanchez, R.A. Allen, K.R. Morrison, K.J. Sommers, R.G. Carden, W.M. Wuest, K.P.C. Minbiole, ChemMedChem 15 (2020) 667.
[48] T.N. Pashirova, A.Y. Ziganshina, E.D. Sultanova, S.S. Lukashenko, Y.R. Kudryashova, E.P. Zhiltsova, L.Y. Zakharova, A.I. Konovalov, Colloids Surf., A 448 (2014) 67.
[49] T.N. Pashirova, A.S. Sapunova, S.S. Lukashenko, E.A. Burilova, A.P. Lubina, Z.M. Shaihutdinova, T.P. Gerasimova, V.I. Kovalenko, A.D. Voloshina, E.B. Souto, L.Y. Zakharova, Int. J. Pharm. 575 (2020) 118953.
[50] E.A. Burilova, T.N. Pashirova, S.S. Lukashenko, A.S. Sapunova, A.D. Voloshina, E. P. Zhiltsova, J.R. Campos, E.B. Souto, L.Y. Zakharova, J. Mol. Liq. 272 (2018) 722.
[51] E.P. Zhiltsova, T.N. Pashirova, R.R. Kashapov, N.K. Gaisin, O.I. Gnezdilov, S.S. Lukashenko, A.D. Voloshina, N.V. Kulik, V.V. Zobov, L.Y. Zakharova, A.I. Konovalov, Russ. Chem. Bull. 61 (2012) 113.
[52] T.N. Pashirova, E.A. Burilova, S.S. Lukashenko, N.K. Gaysin, O.I. Gnezdilov, A.S. Sapunova, A.R. Fernandes, A.D. Voloshina, E.B. Souto, E.P. Zhiltsova, L.Y. Zakharova, J. Mol. Liq. 296 (2019) 112062.
[53] Y. Wang, Z. Liang, Y. Zheng, A.-S.-L. Leung, S.-C. Yan, P.-K. So, Y.-C. Leung, W.-L. Wong, K.-Y. Wong, RSC Adv. 11 (2021) 18122.
[54] I.P. Romanova, A.V. Bogdanov, I.A. Izdelieva, V.A. Trukhanov, G.R. Shaikhutdinova, D.G. Yakhvarov, S.K. Latypov, V.F. Mironov, V.A. Dyakov, I.V. Golovnin, D.Y. Paraschuk, O.G. Sinyashin, Beilstein J. Org. Chem. 10 (2014) 1121.
[55] R. Shimazawa, M. Kuriyama, R. Shirai, Bioorg. Med. Chem. Lett. 18 (2008) 3350.
[56] A.V. Bogdanov, M.E. Kadomtseva, S.V. Bukharov, A.D. Voloshina, V.F. Mironov, Russ. J. Org. Chem. 56 (2020) 555.
[57] J.R. McElhanon, T. Zifer, S.R. Kline, D.R. Wheeler, D.A. Loy, G.M. Jamison, T.M. Long, K. Rahimian, B.A. Simmons, Langmuir 21 (2005) 3259.
[58] A.D. Voloshina, S.K. Gumerova, A.S. Sapunova, N.V. Kulik, A.B. Mirgorodskaya, A.A. Kotenko, T.M. Prokopyeva, V.A. Mikhailov, L.Y. Zakharova, O.G. Sinyashin, Biochimica et Biophysica Acta (BBA) - General Subjects 1864 (2020) 129728.
[59] G.V. Born, Nature 194 (1962) 927.
[60] M.J. Rosen, M. Dahanayake, A.W. Cohen, Colloids Surf. 5 (1982) 159.
[61] P.K. Jana, S.P. Moulik, The Journal of Physical Chemistry 95 (1991) 9525.
[62] R. Zana, J. Colloid Interface Sci. 248 (2002) 203.
[63] H.B. Klevens, 30 (1953) 74.
[64] A. Cornellas, L. Perez, F. Comelles, I. Ribosa, A. Manresa, M.T. Garcia, J. Colloid Interface Sci. 355 (2011) 164.
[65] Q.Q. Baltazar, J. Chandawalla, K. Sawyer, J.L. Anderson, Colloids Surf., A 302 (2007) 150.
[66] M.J. Rosen, J.H. Mathias, L. Davenport, Langmuir 15 (1999) 7340.
[67] L.D. Song, M.J. Rosen, Langmuir 12 (1996) 1149.
[68] M.J. Rosen, L. Liu, Journal of the American Oil Chemists' Society 73 (1996) 885.
[69] K. Tsubone, Y. Arakawa, M.J. Rosen, J. Colloid Interface Sci. 262 (2003) 516.
[70] J. Haldar, V.K. Aswal, P.S. Goyal, S. Bhattacharya, J. Phys. Chem. B 108 (2004) 11406.
[71] R.R. Kashapov, Y.S. Razuvayeva, A.Y. Ziganshina, R.K. Mukhitova, A.S. Sapunova, A.D. Voloshina, L.Y. Zakharova, Colloids Surf., B 175 (2019) 351.
[72] T.N. Pashirova, A.V. Bogdanov, L.I. Musin, J.K. Voronina, I.R. Nizameev, M.K. Kadirov, V.F. Mironov, L.Y. Zakharova, S.K. Latypov, O.G. Sinyashin, Beilstein J Nanotechnol 8 (2017) 313.
[73] J. Woch, J. Iłowska, Z. Hordyjewicz-Baran, S. Arabasz, B. Kaczmarczyk, R. Grabowski, M. Libera, A. Dworak, B. Trzebicka, Soft Matter 14 (2018) 754.
[74] R. Wansri, A.C.K. Lin, J. Pengon, S. Kamchonwongpaisan, N. Srimongkolpithak, R. Rattanajak, P. Wilasluck, P. Deetanya, K. Wangkanont, K. Hengphasatporn, Y. Shigeta, J. Liangsakul, A. Suroengrit, S. Boonyasuppayakorn, T. Chuanasa, W. De-Eknamkul, S. Hannongbua, T. Rungrotmongkol, S. Chamni, Molecules (Basel, Switzerland) 27 (2022).
[75] Y.P. Juang, Y.T. Chou, R.X. Lin, H.H. Ma, T.L. Chao, J.T. Jan, S.Y. Chang, P.H. Liang, Eur. J. Med. Chem. 235 (2022) 114295.
[76] I. Yu Strobykina, A.D. Voloshina, O.V. Andreeva, A.S. Sapunova, A.P. Lyubina, S. K. Amerhanova, M.G. Belenok, L.F. Saifina, V.E. Semenov, V.E. Kataev, Bioorg. Chem. 116 (2021) 105328.
[77] S.K. Amerkhanova, A.D. Voloshina, A.B. Mirgorodskaya, A.P. Lyubina, D.A. Kuznetsova, R.A. Kushnazarova, V.A. Mikhailov, L.Y. Zakharova, Int. J. Mol. Sci. 22 (2021).
[78] T.N. Pashirova, S.S. Lukashenko, S.V. Zakharov, A.D. Voloshina, E.P. Zhiltsova, V. V. Zobov, E.B. Souto, L.Y. Zakharova, Colloids and surfaces, B, Biointerfaces 127 (2015) 266.